

UC Irvine

UC Irvine Previously Published Works

Title

Magnetic and Electronic Properties of URu₂Si₂ Revealed by Comparison with Nonmagnetic References ThRu₂Si₂ and LaRu₂Si₂

Permalink

<https://escholarship.org/uc/item/7nt9b64p>

Journal

Journal of the Physical Society of Japan, 84(6)

ISSN

0031-9015

Authors

Emi, Naoya
Hamabata, Ryosuke
Nakayama, Daisuke
[et al.](#)

Publication Date

2015-06-15

DOI

10.7566/jpsj.84.063702

Copyright Information

This work is made available under the terms of a Creative Commons Attribution License, available at <https://creativecommons.org/licenses/by/4.0/>

Peer reviewed

Magnetic and Electronic Properties of URu₂Si₂ Revealed by Comparison with Nonmagnetic References ThRu₂Si₂ and LaRu₂Si₂

Naoya Emi¹, Ryosuke Hamabata¹, Daisuke Nakayama¹, Toshihiro Miki¹,
Takehide Koyama¹, Koichi Ueda¹, Takeshi Mito^{1*}, Yoh Kohori², Yuji Matsumoto³,
Yoshinori Haga⁴, Etsuji Yamamoto⁴, Zachary Fisk^{4,5}, and Naohito Tsujii⁶

¹Graduate School of Material Science, University of Hyogo, Kamigori, Hyogo 678-1297, Japan

²Graduate School of Science, Chiba University, Chiba 263-8522, Japan

³Graduate School of Engineering, Nagoya Institute of Technology, Nagoya 466-8555, Japan

⁴Advanced Science Research Center, Japan Atomic Energy Agency, Tokai, Ibaraki 319-1195, Japan

⁵University of California, Irvine, CA 92697, U.S.A.

⁶National Institute for Materials Science, Tsukuba, Ibaraki 305-0047, Japan

(Received March 19, 2015; accepted March 30, 2015; published online April 28, 2015)

We have carried out nuclear magnetic resonance (NMR) and nuclear quadrupole resonance (NQR) measurements on ThRu₂Si₂ and LaRu₂Si₂, which are the nonmagnetic references of the intriguing heavy fermion URu₂Si₂. The comparisons of URu₂Si₂ with the reference materials allow us to analyze the already known NMR and NQR data on URu₂Si₂ phenomenologically and semiquantitatively. The study of ¹⁰¹Ru-NQR frequency suggests the relatively close electronic configuration of URu₂Si₂, including the valence of the actinide ion, to that of the tetravalent ThRu₂Si₂ at high temperatures, as well as the delocalization of 5*f* electrons at low temperatures. Ising-like spin fluctuations along the *c*-axis were brought to light by ²⁹Si-NMR data in the so-called hidden order phase of URu₂Si₂. The unique magnetic property is plausibly associated with the mechanism of the unconventional superconductivity.

The uranium heavy fermion URu₂Si₂ has been attracting much interest since its discovery almost 30 years ago¹⁻³⁾ because of its fascinating properties, including the mysterious phase transition at $T_{\text{HO}} = 17.5$ K, whose order parameter has not been identified [so-called “hidden order (HO)”], and its unconventional superconductivity below $T_c = 1.4$ K. Among a wide variety of experimental reports on this compound, studies using nuclear magnetic resonance (NMR) have played an important role in providing microscopic information on the issues of the HO and superconducting phases: for example, a decrease in the density of states at Fermi energy^{4,5)} and spurious antiferromagnetic ordering⁶⁾ in the HO phase, and the existence of line nodes in superconducting energy gap.^{4,5)} Moreover, symmetry changes across the HO have recently been discussed from the magnetic⁷⁻⁹⁾ and electronic¹⁰⁾ points of view.

However, we have noticed that some pieces of fundamental information on magnetic fluctuations and U-valence have been missing owing to the lack of comparisons between the NMR data of URu₂Si₂ and its nonmagnetic references so far. In this paper, we report on the results of NMR and nuclear quadrupole resonance (NQR) measurements performed on the two isostructural non-*f* compounds ThRu₂Si₂ and LaRu₂Si₂. The comparisons of already reported NMR and NQR data on URu₂Si₂^{4,5)} with the present results allow us to analyze them semiquantitatively and to extract unique information on the magnetic and electronic properties of URu₂Si₂. First, we discuss whether ThRu₂Si₂ is suitable as the nonmagnetic reference of URu₂Si₂ on the basis of the NQR data measured at the Ru site. The NQR frequency ν_Q sensitively reflects local charge distribution. Then, by comparing the nuclear spin lattice relaxation rate $1/T_1$ data of URu₂Si₂ with those of ThRu₂Si₂, we conclude that there exist only spin fluctuations along the crystal *c*-axis in the HO phase and these Ising-like fluctuations may be important for the appearance of the unconventional superconductivity in URu₂Si₂.

The single crystals of ThRu₂Si₂ were grown in a tetra-arc furnace under high-purity Ar gas atmosphere by the Czochralski method. The details of the sample preparation are described elsewhere.¹¹⁾ A single crystal sample was used for the estimation of the temperature dependence of ν_Q at the Ru site by ⁹⁹Ru-NMR measurement. Most of other the ²⁹Si-NMR (nuclear spin $^{29}I = 1/2$), ^{99,101}Ru-NMR (^{99,101} $I = 5/2$), and ¹⁰¹Ru-NQR measurements on ThRu₂Si₂ were performed using a powdered sample. A polycrystalline sample of LaRu₂Si₂ was also synthesized by arc-melting constituent elements in Ar atmosphere, and we measured the ¹⁰¹Ru-NQR spectra of this sample. All the NMR and NQR experiments were carried out by the spin-echo technique with a phase-coherent pulsed spectrometer. T_1 was measured by a single rf-pulse saturation method.

The U ion in URu₂Si₂ has been regarded to be between U³⁺ ($5f^3$) and U⁴⁺ ($5f^2$) configurations. Actually, many theoretical models to explain the various properties of URu₂Si₂ seem based on the regime starting from the $5f^2$ configuration.¹²⁾ However, it is difficult to distinguish experimentally these two valences. One of the reasons is that the two 5*f* electron states have quite close values of effective moment (3.62 and 3.58 μ_B for U³⁺ and U⁴⁺, respectively), whose magnetic responses are indistinguishable. Therefore, we focused on the data on ν_Q , which is sensitive to local charge distribution.

Figure 1(a) shows a field-swept ⁹⁹Ru-NMR line of ThRu₂Si₂. The spectrum consists of two peaks around 12.0 T arising from a transition between the nuclear spin states of $-1/2 \leftrightarrow 1/2$ and the two quadrupole-split first satellite lines ($\pm 1/2 \leftrightarrow \pm 3/2$) of ⁹⁹Ru-NMR. An additional resonance peak indicated by an arrow is assigned to one of the two first satellites of ¹⁰¹Ru-NMR. From the obtained spectrum, we were able to extract $^{99}\nu_Q = 1.046$ MHz for the ⁹⁹Ru nucleus, yielding $^{101}\nu_Q = 6.05$ MHz for the ¹⁰¹Ru nucleus using the ratio of nuclear quadrupole moments, $^{101}Q/^{99}Q = 457/79$.¹³⁾ This estimation was verified by the

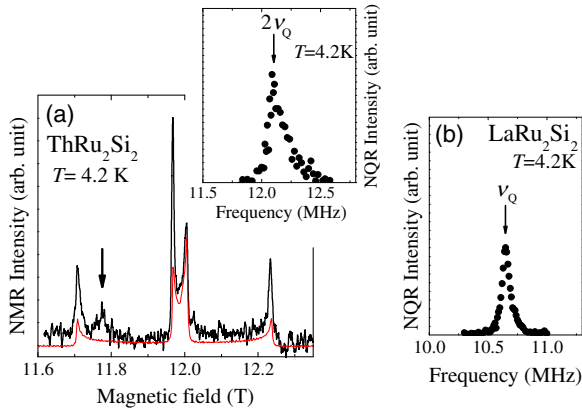


Fig. 1. (Color online) (a) Ru-NMR spectrum of ThRu_2Si_2 measured at 4.2 K and a frequency of 23.56 MHz. The solid line shows a calculated spectrum with ${}^{99}\nu_Q = 1.046$ MHz. The peak indicated by the arrow is assigned to one of the two first satellites of ${}^{101}\text{Ru}$ -NMR. Inset: ${}^{101}\text{Ru}$ -NQR spectrum measured at 4.2 K and a frequency corresponding to a $\pm 3/2 \leftrightarrow \pm 5/2$ transition, i.e., $2 \times {}^{101}\nu_Q$. (b) ${}^{101}\text{Ru}$ -NQR spectrum of LaRu_2Si_2 measured at 4.2 K and ${}^{101}\nu_Q$. The measurement of the ${}^{101}\text{Ru}$ -NQR spectrum was performed at ${}^{101}\nu_Q$ because the spectrum at $2 \times {}^{101}\nu_Q$ overlaps with the tail of the $3 \times {}^{139}\nu_Q$ line of ${}^{139}\text{La}$ -NQR with $I = 7/2$ and ${}^{139}\nu_Q = 7.01$ MHz.

observation of a ${}^{101}\text{Ru}$ -NQR signal at a frequency of 12.1 MHz = $2 \times {}^{101}\nu_Q$, as shown in the inset of Fig. 1(a). At the Ru site with fourfold symmetry along the c -axis, the ratio of NQR frequencies $\nu_Q : \nu_Q(2) = 1 : 2$, where ν_Q and $\nu_Q(2)$ are resonance frequencies for the transitions between $\pm 1/2 \leftrightarrow \pm 3/2$ and $\pm 3/2 \leftrightarrow \pm 5/2$, respectively.

Note that the ${}^{101}\nu_Q$ of URu_2Si_2 [${}^{101}\nu_Q(\text{URu}_2\text{Si}_2) = 5.72$ MHz^{5,10,14}] is close to that of ThRu_2Si_2 [${}^{101}\nu_Q(\text{ThRu}_2\text{Si}_2) = 6.05$ MHz] in which the Th ion is tetravalent. Actually, it is difficult to estimate ionic valence quantitatively only from the ν_Q data. However, if we see how ν_Q changes in valence transition or valence-fluctuating systems (see, for example, Ref. 15 and the case of YbPd_2Si_2 described below), the present small difference in ${}^{101}\nu_Q$ (~ 0.3 MHz) between URu_2Si_2 and ThRu_2Si_2 suggests the similarity of electronic configuration, except for $5f$ electrons, between the two compounds.

${}^{101}\nu_Q(\text{ThRu}_2\text{Si}_2)$ shows weak temperature dependence, as shown in Fig. 2(a). A more precise temperature dependence of ${}^{101}\nu_Q$ was measured for LaRu_2Si_2 in order to obtain further information on electronic states in URu_2Si_2 . ${}^{101}\nu_Q(\text{LaRu}_2\text{Si}_2)$ estimated as 10.65 MHz at 4.2 K [see Fig. 1(b)] is close to ${}^{101}\nu_Q = 10.52$ MHz for CeRu_2Si_2 ,¹⁶ both of which are trivalent or quasitrivalent compounds. On the other hand, ${}^{101}\nu_Q(\text{LaRu}_2\text{Si}_2)$ is ~ 1.9 times larger than ${}^{101}\nu_Q(\text{ThRu}_2\text{Si}_2)$. The difference is predominantly attributed to the difference in the charge distribution between the two systems. This result also supports the fact that the U valence is closer to 4+ rather than 3+, so that we found that ThRu_2Si_2 is applicable as the nonmagnetic reference of URu_2Si_2 .

One should also notice that the temperature dependence of ${}^{101}\nu_Q(\text{URu}_2\text{Si}_2)$ contrasts with that of ${}^{101}\nu_Q(\text{LaRu}_2\text{Si}_2)$. ${}^{101}\nu_Q(\text{LaRu}_2\text{Si}_2)$ shows a gradual decrease with increasing temperature, as seen in the upper panel of Fig. 2(a), which is a characteristic behavior reflecting a normal thermal expansion of the lattice. The result suggests that no significant rearrangement of charge distribution occurs with

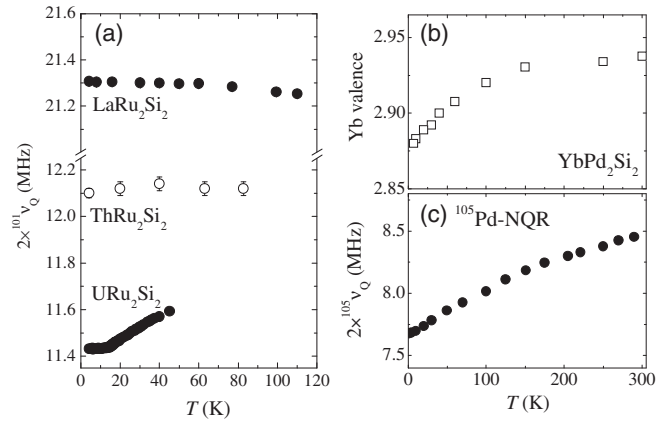


Fig. 2. (a) Temperature dependences of $2 \times {}^{101}\nu_Q$ for URu_2Si_2 ,¹⁰ LaRu_2Si_2 , and ThRu_2Si_2 . The ThRu_2Si_2 data for $T \geq 20$ K were estimated from ${}^{99}\text{Ru}$ -NMR measurement of a single crystal owing to the poor signal intensity of ${}^{101}\text{Ru}$ -NQR. Other data were obtained from ${}^{101}\text{Ru}$ -NQR measurements. (b) Temperature dependence of the Yb valence of the valence-fluctuating compound YbPd_2Si_2 evaluated from X-ray absorption spectroscopy measurement.¹⁷ (c) Temperature dependence of $2 \times {}^{105}\nu_Q$ obtained from the ${}^{105}\text{Pd}$ -NQR measurement.

temperature, namely, the La ion is in a stable trivalent state. In this context, we may expect a somewhat similar temperature dependence for ${}^{101}\nu_Q(\text{ThRu}_2\text{Si}_2)$ as well.

On the other hand, ${}^{101}\nu_Q(\text{URu}_2\text{Si}_2)$ increases with temperature above T_{HO} . Therefore, the difference between ${}^{101}\nu_Q(\text{URu}_2\text{Si}_2)$ and ${}^{101}\nu_Q(\text{ThRu}_2\text{Si}_2)$ (~ 0.3 MHz at 4.2 K as mentioned above) is even smaller at higher temperatures, suggesting a closer electronic configuration between these two compounds at high temperatures. The decrease in ν_Q in the low-temperature region is generally observed in valence-fluctuating lanthanide compounds, where the positive valence of lanthanide ions simultaneously decreases upon cooling. We found that the temperature dependence of ${}^{101}\nu_Q(\text{URu}_2\text{Si}_2)$ is analogous to that of the isostructural Yb compound YbPd_2Si_2 . Here, the Yb valence was studied by X-ray absorption spectroscopy,¹⁷ as shown in Fig. 2(b). As temperature decreases, the delocalization of $4f$ electrons is induced owing to the evolution of exchange interactions between conduction and $4f$ electrons, resulting in the decrease in the Yb valence (valence-fluctuating state) and simultaneously in $\nu_Q(\text{YbPd}_2\text{Si}_2)$ [see Fig. 2(c)]. Similarly, the temperature dependence of ${}^{101}\nu_Q(\text{URu}_2\text{Si}_2)$ revealed in Fig. 2(a) suggests the delocalization of U- $5f$ electrons at low temperatures. For a more quantitative discussion, reliable theoretical calculations are required.

Next, we show the results of ${}^{29}\text{Si}$ -NMR measurements. The ${}^{29}\text{Si}$ -NMR line exhibits a slightly asymmetric powder pattern, as seen in Fig. 3, implying that it consists of small anisotropic components of the Knight shift K . However, the evaluated anisotropic component of the shift is quite small: $K_{\text{aniso}} = 8 \times 10^{-3}\%$. Therefore, compared with the strongly anisotropic Knight shift of URu_2Si_2 ,⁴ the shift is regarded to be almost isotropic. As discussed in Ref. 4, the hyperfine coupling constant of URu_2Si_2 is isotropic, and the present results are consistent with this.

By measuring the intensities of the ${}^{29}\text{Si}$ -NMR signal near the frequencies indicated by arrows in Fig. 3, we could estimate $1/T_1$ of ThRu_2Si_2 [hereafter denoted as ${}^{\text{Th}}(1/T_1)$]

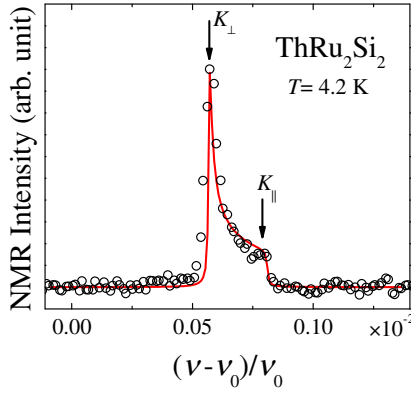


Fig. 3. (Color online) Fourier-transformed spectrum of ^{29}Si -NMR measured at 4.2 K and an external field of $H_0 = 5.9998$ T. The horizontal axis indicates the evaluated shift, where $\nu_0 = {}^{29}\gamma_n/2\pi \times H_0$ with ${}^{29}\gamma_n/2\pi = 8.4577$ MHz/T. The signal intensity near the frequency regions indicated by arrows was used to estimate T_1 components for $H \parallel c$ and $H \perp c$.

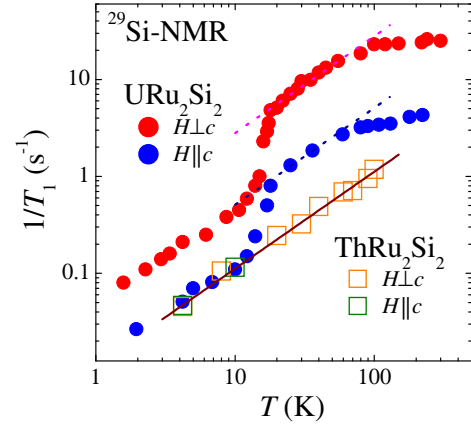


Fig. 4. (Color online) Temperature dependence of $1/T_1$ measured by ^{29}Si -NMR. The previous data of URu_2Si_2 ⁴⁾ are compared with the present results for ThRu_2Si_2 . The solid line is a linear fit to the data for $H \perp c$, and the broken lines indicate Korringa-like behavior for URu_2Si_2 above T_{HO} .

for $H \parallel c$ and $H \perp c$, i.e., ${}^{\text{Th}}(1/T_1)_{\parallel}$ and ${}^{\text{Th}}(1/T_1)_{\perp}$, respectively. Their temperature dependences are shown in Fig. 4, along with the previously reported data on URu_2Si_2 [${}^{\text{U}}(1/T_1)$].⁴⁾ ${}^{\text{Th}}(1/T_1)_{\perp}$ shows the so-called Korringa relation

$${}^{\text{Th}}(1/T_1)_{\perp} = 0.0112T, \quad (1)$$

which is a characteristic behavior of a Fermi liquid. Although we were able to measure ${}^{\text{Th}}(1/T_1)_{\parallel}$ only up to 10 K owing to a poor signal-to-noise ratio, the result indicates that ${}^{\text{Th}}(1/T_1)$ is isotropic within experimental accuracy. For $T > T_{\text{HO}}$, we assume that Eq. (1) corresponds to a contribution from conduction electrons without $5f$ electrons in URu_2Si_2 . As indicated in Ref. 4, ${}^{\text{U}}(1/T_1)$ shows the Korringa relation above T_{HO} , as shown by dotted lines in Fig. 4. Since $1/T_1 T$ is generally proportional to $D(\epsilon_F)^2$, with $D(\epsilon_F)$ being the density of states at Fermi energy, the enhancement of ${}^{\text{U}}(1/T_1)$ compared with ${}^{\text{Th}}(1/T_1)$ above T_{HO} implies the formation of a heavy Fermi liquid owing to the Kondo effect.

A remarkable feature shown in Fig. 4 is that ${}^{\text{U}}(1/T_1)_{\parallel}$ abruptly decreases to the line expressed by Eq. (1) below T_{HO} . $(1/T_1)_{\parallel}$ and $(1/T_1)_{\perp}$ are related to the dynamical susceptibilities perpendicular and parallel to the c -axis, $\chi_{\perp}(q, \omega_0)$ and $\chi_{\parallel}(q, \omega_0)$, respectively, as follows:

$$\left(\frac{1}{T_1}\right)_{\parallel} = \frac{2\gamma_n^2 k_B T}{(\gamma_e \hbar)^2} \sum_q \left[A_{\text{hf},\perp}^2 \frac{\text{Im} \chi_{\perp}(q, \omega_0)}{\omega_0} \right], \quad (2)$$

and

$$\left(\frac{1}{T_1}\right)_{\perp} = \frac{\gamma_n^2 k_B T}{(\gamma_e \hbar)^2} \sum_q \left[A_{\text{hf},\parallel}^2 \frac{\text{Im} \chi_{\parallel}(q, \omega_0)}{\omega_0} + A_{\text{hf},\perp}^2 \frac{\text{Im} \chi_{\perp}(q, \omega_0)}{\omega_0} \right], \quad (3)$$

where γ_n and γ_e are the nuclear and electronic gyromagnetic ratios, respectively, ω_0 is the NMR frequency, $\text{Im} \chi_i(q, \omega_0)$ is the imaginary part of $\chi_i(q, \omega_0)$ ($i = \parallel$ and \perp), and $A_{\text{hf},\parallel} \approx A_{\text{hf},\perp}$ for URu_2Si_2 and ThRu_2Si_2 , as mentioned above. From Eq. (2), the decrease in ${}^{\text{U}}(1/T_1)_{\parallel}$ below T_{HO} implies that $\chi_{\perp}(q, \omega_0)$ in the HO phase is as small as that in the nonmagnetic metal ThRu_2Si_2 .

On the other hand, $(1/T_1)_{\perp}$ predominantly obtains contribution from $\chi_{\parallel}(q, \omega_0)$, because $\chi_{\perp}(q, \omega_0)$ is small in Eq. (3). The anisotropy in ${}^{\text{U}}(1/T_1)$, which is in contrast to the

case of ThRu_2Si_2 , indicates the existence of magnetic correlations between electrons even in the Fermi liquid state. Therefore, the enhancement of ${}^{\text{U}}(1/T_1)_{\perp}$ in the HO phase is ascribed to the spin fluctuations existing only along the c -axis. Such a unique observation in URu_2Si_2 should be associated with the Ising-like magnetic property, which is revealed for example in the strongly anisotropic susceptibility: the magnetic signal along the a -axis is almost temperature-independent and several times smaller than that along the easy axis (c -axis).¹⁾

We briefly comment on the appearance of the superconductivity in URu_2Si_2 . The superconductivity occurs in the lower-temperature region included by the HO phase having the Ising-type magnetic fluctuations, as mentioned above. If Cooper pairing is magnetically mediated there, the spin fluctuations along the c -axis should be responsible for the superconductivity, because the perpendicular component as small as those in ThRu_2Si_2 is unlikely to be the main driving force for the occurrence of the unconventional, anisotropic superconductivity. This regime is also consistent with the strong anisotropy in the upper critical field H_{c2} ¹⁸⁾ [i.e., $H_{c2}(H \perp c) > H_{c2}(H \parallel c)$]: spin fluctuations will be considerably suppressed when applying magnetic field along the c -axis, leading to the depression of the superconductivity. Interestingly, a similar Ising anisotropy characterizes the magnetic properties in the U-based ferromagnetic (FM) superconductors URhGe and UCoGe ,^{19,20)} in which FM fluctuations are intimately related to the appearance of superconductivity.²¹⁾

Further information on the spin fluctuations detected by the present T_1 measurements is obtained using the modified Korringa relation for weakly correlated metals: $T_1 T K_s^2 = SK(\alpha)^{-1}$, where K_s is the spin part of K , $S = \hbar/4\pi k_B (\gamma_e/\gamma_n)^2$, $K(\alpha) = (1 - \alpha)^2 [1 - \alpha(\chi_0(q)/\chi_0(0))]^{-2}$, $(1 - \alpha)^{-1}$ is an enhancement factor, and $\chi_0(q)$ is the dynamical susceptibility for noninteracting fermions.²²⁾ At low temperatures in the HO phase, $K_{s,\parallel} = 0.31\%$,²³⁾ being independent of temperature. Note that $K_{s,\parallel} \propto \chi_{\parallel}(0, 0)$, and $\chi_{\parallel}(q, \omega_0)$ is probed by ${}^{\text{U}}(1/T_1)_{f,\perp} - {}^{\text{U}}(1/T_1)_{f,\parallel}/2$ from Eqs. (2) and (3), where ${}^{\text{U}}(1/T_1)_{f,i}$ ($i = \perp$ and \parallel) denotes $5f$ electronic components. Although ${}^{\text{U}}(1/T_1)_{f,i}$ may be extracted by subtracting the contribution of conduction electrons, it is indeed difficult to

estimate it correctly in the HO phase, because one needs to consider the reduction in carrier density below T_{HO} . Here, if we assume $U(1/T_1)_{f,i} \sim U(1/T_1)_i - \text{Th}(1/T_1)_i$, which should give a lower limit of $U(1/T_1)_{f,i}$, we obtain $K(\alpha) \ll 1$ for $H \parallel c$. This result does not vary even if we assume $U(1/T_1)_{f,i} \sim U(1/T_1)_i$, which should give an upper limit.

According to the modified Korringa relation, the result indicates FM correlations in the HO phase. On the other hand, one expects antiferromagnetic (AFM) correlations originating from the neighboring AFM order phase under pressure. Indeed, a magnetic excitation with the AFM wave vector $Q_0 = (1, 0, 0)$ was detected by an inelastic neutron measurement.²⁴⁾ Here, to understand the present NMR result, we need to take into account the crystallographical surroundings of the Si site: it is located near an *ab* basal plane with four nearest-neighbor U ions. As expected from the Q_0 vector, the U magnetic moments tend to align ferromagnetically within the *ab* basal plane, so that they give rise to FM fluctuations that cannot be canceled out at the Si site. Thus, the T_1 relaxation is predominantly affected by the FM correlations owing to the geometrical factor; thus, the present result is not in disagreement with the AFM correlations between the planes.

In summary, the comparisons of already reported NMR and NQR data on URu₂Si₂ with the data on isostructural nonmagnetic references (ThRu₂Si₂ and LaRu₂Si₂) and a valence-fluctuating compound (YbPd₂Si₂) have uncovered some electronic and magnetic properties of URu₂Si₂. The data on $^{101}\nu_Q$ and its temperature dependence suggest that the U electronic configuration is close to $5f^2$ at high temperatures, while the $5f$ electrons gradually delocalize with decreasing temperature. From the $1/T_1$ data of ^{29}Si -NMR, we found Ising-like spin fluctuations along the *c*-axis in the HO phase. The unique magnetic property is plausibly associated with the mechanism of unconventional superconductivity.

Acknowledgements We thank K. Ishida, Y. Takahashi, H. Harima, G. Motoyama, M. Mizumaki, and T. Kohara for valuable discussions. This work was partially supported by JSPS KAKENHI Grant No. 24540349.

*mito@sci.u-hyogo.ac.jp

- 1) T. T. M. Palstra, A. A. Menovsky, J. van den Berg, A. J. Dirkmaat, P. H. Kes, G. J. Nieuwenhuys, and J. A. Mydosh, *Phys. Rev. Lett.* **55**, 2727 (1985).
- 2) W. Schlabitz, J. Baumann, B. Pollit, U. Rauchschwalbe, H. M. Mayer, U. Ahlheim, and C. D. Bredl, *Z. Phys. B* **62**, 171 (1986).
- 3) M. B. Maple, J. W. Chen, Y. Dalichaouch, T. Kohara, C. Rossel, M. S. Torikachvili, M. W. McElfresh, and J. D. Thompson, *Phys. Rev. Lett.* **56**, 185 (1986).
- 4) Y. Kohori, K. Matsuda, and T. Kohara, *J. Phys. Soc. Jpn.* **65**, 1083

- (1996).
- 5) K. Matsuda, Y. Kohori, and T. Kohara, *J. Phys. Soc. Jpn.* **65**, 679 (1996).
- 6) K. Matsuda, Y. Kohori, T. Kohara, K. Kuwahara, and H. Amitsuka, *Phys. Rev. Lett.* **87**, 087203 (2001).
- 7) S. Takagi, S. Ishihara, M. Yokoyama, and H. Amitsuka, *J. Phys. Soc. Jpn.* **81**, 114710 (2012).
- 8) S. Kambe, Y. Tokunaga, H. Sakai, T. D. Matsuda, Y. Haga, Z. Fisk, and R. E. Walstedt, *Phys. Rev. Lett.* **110**, 246406 (2013).
- 9) K. R. Shirer, J. T. Haraldsen, A. P. Dioguardi, J. Crocker, N. apRoberts-Warren, A. C. Shockley, C.-H. Lin, D. M. Nisson, J. C. Cooley, M. Janoschek, K. Huang, N. Kanchanavatee, M. B. Maple, M. J. Graf, A. V. Balatsky, and N. J. Curro, *Phys. Rev. B* **88**, 094436 (2013).
- 10) T. Mito, M. Hattori, G. Motoyama, Y. Sakai, T. Koyama, K. Ueda, T. Kohara, M. Yokoyama, and H. Amitsuka, *J. Phys. Soc. Jpn.* **82**, 123704 (2013).
- 11) Y. Matsumoto, Y. Haga, N. Tateiwa, H. Aoki, N. Kimura, T. D. Matsuda, E. Yamamoto, Z. Fisk, and H. Yamagami, *JPS Conf. Proc.* **3**, 011096 (2014).
- 12) For a review, see J. A. Mydosh and P. M. Oppenher, *Rev. Mod. Phys.* **83**, 1301 (2011).
- 13) P. Pyykkö, *Mol. Phys.* **106**, 1965 (2008).
- 14) S. Saitoh, S. Takagi, M. Yokoyama, and H. Amitsuka, *J. Phys. Soc. Jpn.* **74**, 2209 (2005).
- 15) For example, in the valence transition compound YbInCu₄, ν_Q of ^{63}Cu changes by $\sim 0.8 \text{ MHz}^{25,26}$ across the Yb valence change from 2.98 (high-temperature phase) to 2.84 (low-temperature phase).²⁷⁾ Note that ν_Q is in proportion to QV_{zz} , where Q is the nuclear quadrupole moment ($^{63}\text{Q} = -0.211 \times 10^{-24} \text{ cm}^2$ and $^{101}\text{Q} = -0.45 \times 10^{-24} \text{ cm}^2$) and V_{zz} is the largest principal axis component of the electric field gradient at the nuclear position.
- 16) Y. Kawasaki, Dr. Thesis, Osaka University, 1998.
- 17) H. Yamaoka, I. Jarrige, N. Tsujii, J.-F. Lin, N. Hiraoka, H. Ishii, and K.-D. Tsuei, *Phys. Rev. B* **82**, 035111 (2010).
- 18) D. Aoki, F. Bourdarot, E. Hassinger, G. Knebel, A. Miyake, S. Raymond, V. Taufour, and J. Flouquet, *J. Phys.: Condens. Matter* **22**, 164205 (2010), and references therein.
- 19) D. Aoki, A. Huxley, E. Ressouche, D. Braithwaite, J. Flouquet, J.-P. Brison, E. Lhotel, and C. Paulsen, *Nature* **413**, 613 (2001).
- 20) N. T. Huy, D. E. de Nijs, Y. K. Huang, and A. de Visser, *Phys. Rev. Lett.* **100**, 077002 (2008).
- 21) T. Hattori, Y. Ihara, Y. Nakai, K. Ishida, Y. Tada, S. Fujimoto, N. Kawakami, E. Osaki, K. Deguchi, N. K. Sato, and I. Satoh, *Phys. Rev. Lett.* **108**, 066403 (2012).
- 22) T. Moriya, *J. Phys. Soc. Jpn.* **18**, 516 (1963).
- 23) For URu₂Si₂, given that the susceptibility at high temperatures can be fitted with a simple Curie Weiss¹⁾ and the plot of K_{\parallel} as a function of the susceptibility extrapolates to the origin,⁴⁾ we approximate $K_{\parallel} \sim K_{s,\parallel}$.
- 24) C. Broholm, H. Lin, P. T. Matthews, T. E. Mason, W. J. L. Buyers, M. F. Collins, A. A. Menovsky, J. A. Mydosh, and J. K. Kjems, *Phys. Rev. B* **43**, 12809 (1991).
- 25) H. Nakamura, K. Nakajima, Y. Kitaoka, K. Asayama, K. Yoshimura, and T. Nitta, *J. Phys. Soc. Jpn.* **59**, 28 (1990).
- 26) T. Koyama, M. Nakamura, T. Mito, S. Wada, and J. L. Sarrao, *Phys. Rev. B* **71**, 184437 (2005).
- 27) S. Suga, A. Sekiyama, S. Imada, J. Yamaguchi, A. Shigemoto, A. Irizawa, K. Yoshimura, M. Yabashi, K. Tamasaku, A. Higashiya, and T. Ishikawa, *J. Phys. Soc. Jpn.* **78**, 074704 (2009).